



# Incorporation effect of inulin and microbial transglutaminase on the gel properties of silver carp (*Hypophthalmichthys molitrix*) surimi

Jianlian Huang<sup>1</sup> · Beibei Ye<sup>2</sup> · Wei Wang<sup>2</sup> · Jianrong Li<sup>2</sup> · Shumin Yi<sup>2</sup> · Xuepeng Li<sup>2</sup> · Yongxia Xu<sup>2</sup> · Hongbo Mi<sup>2</sup>

Received: 27 March 2020 / Accepted: 11 August 2020 / Published online: 25 August 2020  
© Springer Science+Business Media, LLC, part of Springer Nature 2020

## Abstract

Surimi-based products with elasticity and specific shapes have received considerable notice in recent years. To ascertain the effects of inulin, microbial transglutaminase (MTGase) and the combination of inulin/MTGase on gel formation of silver carp surimi, the gel strength, textural properties, water-holding capacity (WHC), dynamic rheological measurements, Raman spectroscopy, light microscopy of gel structure and sodium dodecyl sulfate-polyacrylamide gel electrophoresis (SDS-PAGE) of gels from different groups were analyzed. The results showed that addition of inulin, MTGase and MTGase + inulin improved gel strength (increased by 7.7%, 26.8% and 38.56% compared with control group), textural properties and WHC. Raman spectroscopy proven that MTGase + inulin promoted the conversion of  $\alpha$ -helixes to  $\beta$ -sheets and  $\beta$ -turns compared with other experimental and control groups. Pure surimi gelation contained a loose and non-heterogeneous network via light microscopy. With the addition of MTGase and inulin, the microstructure of surimi gelation became more compact and homogeneous, particularly the MTGase + inulin groups. Moreover, The SDS-PAGE pattern further disclosed that the MTGase + inulin had a weakened myosin heavy chain band, indicating that inulin could enhance the cross-linking effects of MTGase on myosin heavy chains. These data demonstrated inulin incorporating with MTGase may be a new and effective strategy to improve the gel properties of fish surimi.

**Keywords** Silver carp surimi · MTGase · Inulin · Gel property · Synergetic effect

## Introduction

Surimi gel products prepared with minced fish muscle are generally defined as a series of flexible and protein-based processed food. Over the past decade, due to distinct textural properties, nutritional benefits and better edible

convenience, it fulfils a prominent role in consumers' diets. In order to make full use of aquatic resources and meet the needs of people, using freshwater or low-value fish to manufacture raw surimi has long been the focus of aquatic products processing industry. Silver carp (*Hypophthalmichthys molitrix*) is a widely cultured freshwater fish due to low price, fast growth as well as high nutritional value, and its production in 2018 reached 3.858 million tons comprising up to 15.17% of freshwater fish cultured in China [32, 34]. Along with deep processing of silver carp and decreasing of marine fish resources, silver carp become a potential alternative raw material for surimi production [19, 50]. Whereas, like other freshwater fish, silver carp surimi has poor gel-forming ability and unpleasant flavor, which compromising its commercial value [12]. Therefore, improving the gel properties could contribute to the processing and utilization of the freshwater fishes.

In recent years, numerous studies have been carried out that adding appropriate dietary fiber additives including insoluble sugarcane bagasse, nanosized okara dietary fiber,

Co first author: Beibei Ye.

✉ Shumin Yi  
shuminyi@163.com

✉ Xuepeng Li  
xuepengli8234@163.com

<sup>1</sup> Key Laboratory of Refrigeration and Conditioning Aquatic Products Processing, Ministry of Agriculture and Rural Affairs, Xiamen 361026, China

<sup>2</sup> College of Food Science and Engineering, Bohai University, National R & D Branch Center of Surimi and Surimi Products Processing, 19 Keji Road, Jinzhou 121013, Liaoning, China

pea and chicory root fiber, is an effective way for improving the quality of freshwater fish surimi gel during processing [9, 51, 57]. It is well known that due to the prevention effect of diseases such as obesity, diabetes, cardiovascular diseases, etc., and satiety property, dietary fiber has been an issue of great interest in food field [6, 10, 40]. What is more, Alakhrash et al. [2], Debusca et al. [13] and Zhang et al. [52] have reported dietary fiber can act as filler, binders or extender to improve water holding capacity, gel strength, emulsion stability, texture value, sensory characters of processed aquatic products. According to the differences in solubility, dietary fiber is divided into two types, insoluble and soluble fiber. As for gel improver, insoluble dietary fiber has been widely investigated in fish muscle. However, there has been little discussions about the role played by soluble dietary fiber in freshwater fish surimi gel.

Inulin is a soluble dietary fiber composed of 22–60 glucosyl moieties and one fructose unit bounded by  $\beta$ -(2–1) linkage, which presents in a good number of plant resources such as chicory, Jerusalem artichoke, wheat, garlic and so on [28, 35, 53]. It is classified into short-chain, long-chain and natural inulin basing on different degrees of polymerization [36]. At present, inulin has been used as lipid replacer in low-fat healthier food products because of fat-like characteristics. In addition, Kuntz et al. [24] and Shoaib et al. [42] also found that inulin plays an influential role in improving the intestinal environment and balancing the flora. Of interest is that inulin is also capable of forming particle gels with stable network when blended with water or other aqueous phase systems [4]. Xu et al. [48] found that inulin could be as structural and property modifiers for sodium caseinate stabilized oil-in-water emulsions. Kiumarsi et al. [22] also reported when inulin was added into gluten-free bread, it could effectively decrease starch crystallinity and produce a softer crumb. Briefly, inulin and its derivatives added to food formulation become more commonplace in food industry.

Previously, MTGase has been proven to promote the formation of protein cross-linking via  $\epsilon$ -( $\gamma$ -glutamine)-lysine bonds and employed in practical production of various gel products including surimi gel, restructure meat product, yoghurt, etc. [3, 16, 23, 41]. However, there are few references about effects of inulin or the combination of inulin and MTGase on the gel properties of freshwater fish surimi.

Therefore, the objective of the present study was to analyze the synergetic effects of inulin/MTGase surimi batter composites and to explore the regulatory mechanism of inulin on MTGase-induced gel formation of surimi. Herein, we analyzed the changes in gel texture, rheology, secondary structure and protein pattern of silver carp surimi after treatment with inulin, MTGase and inulin + MTGase, to provide data support for the application of inulin/MTGase in surimi products.

## Materials and methods

### Materials

Silver carp (*H. molitrix*) surimi (3A grade, containing 75% water, 16.62% protein, 4.07% fat and 3.81% ash) was obtained from Honghu Jingli Aquatic Food Co., Ltd. (Honghu, China). Food-grade salt was purchased from a local market (Jinzhou, China). Inulin (Orafti@GR, GR, average DP  $\geq$  10) was purchased from Beneo Co., Ltd. (Mannheim, Germany). Microbial transglutaminase (MTGase, 1000 U/g, food grade) was acquired from Nanning Dongheng Huadao Biotechnology Co., Ltd. (Guangxi, China). SiO<sub>2</sub> was purchased from Tianjin Longhua Chemical Co., Ltd. (Tianjin, China).

### Preparation of surimi gels

Silver carp surimi was used with other ingredients in the preparation of gels (Table 1). Briefly, frozen surimi was thawed with flowing water, then chopped at low speed in a vacuum chopper (Model UMC5, Stephan Machinery Corp., Germany) for 1 min. Surimi paste was subsequently obtained by adding 25 g/kg NaCl and chopping for 2 min at low speed. The final moisture content was adjusted to 780 g/kg by adding cold water (4 °C), 10 g/kg inulin and 2.5 g/kg MTGase to the paste. To maintain the same protein concentration and moisture content in all treatments, food-grade inert filler silica (SiO<sub>2</sub>) was added into the surimi paste. All ingredients were mixed with the surimi paste and chopped under vacuum (– 0.6 kPa) for the last 4 min. The paste temperature was controlled at less than 10 °C during chopping.

**Table 1** Surimi batter formulations

Groups	Surimi (g/1000 g)	Water (g/1000 g)	Inulin (g/1000 g)	MTGase (g/1000 g)	SiO <sub>2</sub> (g/1000 g)	Batch weight (g)
Control	730	232.5	0	0	12.5	1000
Inulin	730	232.5	10	0	2.5	1000
MTGase	730	232.5	0	2.5	10	1000
MTGase + inulin	730	232.5	10	2.5	0	1000

Each surimi paste was stuffed into a 45 mm plastic casing and allowed to set at 40 °C for 30 min and then 90 °C for 20 min. The gel was immediately placed in ice water to cool for 15 min. All samples were stored overnight at 4 °C, after which the prepared gel was placed at room temperature for 30 min before analysis.

### Strength of surimi gels

The gel strength was measured using a TA. XT plus texture analyzer (Stable Micro System Corp., UK), and the sample was cut into a cylinder having a diameter of 2.5 cm and a height of 2.5 cm, and were tested using a P/5S probe. The physical property parameters were set to 50% for compression, 10 g for downforce, 1.0 mm/s for pre-test, and 1.0 mm/s for test. The gel sample was placed at room temperature for 30 min before testing.

### Textural properties of surimi gels

To evaluate the texture of the surimi gels, cylindrical gels (length = 2.5 cm, diameter = 2.5 cm) were tested using a TA. XT plus texture analyzer (Stable Micro System Corp., UK) with a P/50 probe. The physical property parameters were set to 50% for compression, 10 g for downforce, 1.0 mm/s for pre-test, and 1.0 mm/s for test. The gel sample was placed at room temperature for 30 min before testing.

### Water holding capacity of surimi gels

The water holding capacity (WHC) was measured using the method described by Sánchez-González et al. [38], with slight modification. Briefly, gel samples were cut into 5 mm slices (about 1.5 g), accurately weighed as W1, and wrapped in a 50 mL centrifuge tube with three layers of filter paper. After centrifugation at 5000 rpm for 15 min at 4 °C, the sample was quickly taken out and accurately weighed, after which the weight was recorded as W2. Each set of samples was run in parallel three times. The WHC was then calculated according to the following formula:

$$\text{WHC (\%)} = \frac{W2}{W1} \times 100, \quad (4)$$

where W1 is the weight of the sample before centrifugation and W2 is the weight of the sample after centrifugation.

### Oscillatory dynamic rheology of surimi gels

The surimi pastes were determined using a dynamic rheometer (DHR-1, TA Instruments Ltd., UK) to simulate the heat-induced gel formation process of the surimi based on the method described by Debusca et al. [14], with slight modification. Briefly, the sample was placed between the lamina

(4° and 40 mm) and the plate at a pitch of 150 μm. The surimi mixture was then heated from 20 to 90 °C at a rate of 1 °C/min with a fixed scanning frequency of 0.1 Hz and a scanning stress of 100 Pa. During the scanning process, the scanning stress was in the linear viscoelastic region.

### Raman spectroscopy of surimi gels

The sample was cut into 2 × 2 × 1 mm and placed on a clean slide. The secondary structure of the protein was determined by a laser Raman spectrometer (LabRAM HR Evolution, Horiba Trading Ltd., China). The laser source is an argon ion laser with the following parameters: laser wavelength 532 nm, power 100%, exposure time 30 s, Raman shift range 400–4000 cm<sup>-1</sup>.

### Light microscopy of surimi gels

The microstructures of MP gels were determined according to Wu et al. [45] with slight modification. Briefly, samples were cut into 5 × 5 × 5 mm pieces and refrigerated at – 80 °C for 20 min. The pieces were then cut into 10 μm slices with a cryostat and placed on a glass slide. Next, slices were stained with hematoxylin–eosin (HE), then observed and photographed using a light microscope (80i, Nikon Ltd., Japan).

### Sodium dodecyl sulfate-polyacrylamide gel electrophoresis of surimi gels

Sodium dodecyl sulfate-polyacrylamide gel electrophoresis (SDS-PAGE) of surimi gels was examined as described by Zhu et al. [54], with slight modifications. Briefly, surimi gel (3.0 g) amended with 27.0 mL of 5% SDS solution (85 °C) was homogenized at 11,000 rpm for 4 min, after which the homogenate was incubated at 85 °C for 1 h to solubilize total proteins. The supernatant was then collected after centrifuging at 10,000 rpm for 20 min to remove undissolved debris. Next, the concentration of supernatant was adjusted to 6 mg/mL and mixed with sample buffer at a ratio of 1:1 (v/v). The mixture was subsequently boiled for 10 min, after which the samples (10 μL) were loaded onto the polyacrylamide gel made of 4% stacking gel and 12% separation gel and subjected to electrophoresis at 80 V for 15 min, then 120 V for 80 min with a constant current. After running, proteins were stained with 0.25% Coomassie Blue R-250, then destained in 50% ethanol and 10% acetic acid. Protein profiles were analyzed using the Quantity One software (BioRad Laboratories, Inc., Richmond, CA, USA).

### Statistical analysis

All statistical analyses of data were performed using the statistical product and service solutions (SPSS) 19.0

software. Data were subjected to one-way analysis of variance (ANOVA). Results were reported as mean values  $\pm$  the standard deviation (SD). A  $P < 0.05$  was considered to indicate significance.

## Results and discussion

### Strength of silver carp surimi gels

Gel strength is defined as the product of breaking force and deformation, providing the evidence of surimi products in grading. The effects of different additives on the strength of silver carp surimi gel are shown in Fig. 1. SiO<sub>2</sub> was added into the surimi to ensure that the protein concentration remained the same. Therefore, the changes in experimental results only reflect changes in inulin and MTGase, not decreases in protein concentration [14]. The breaking

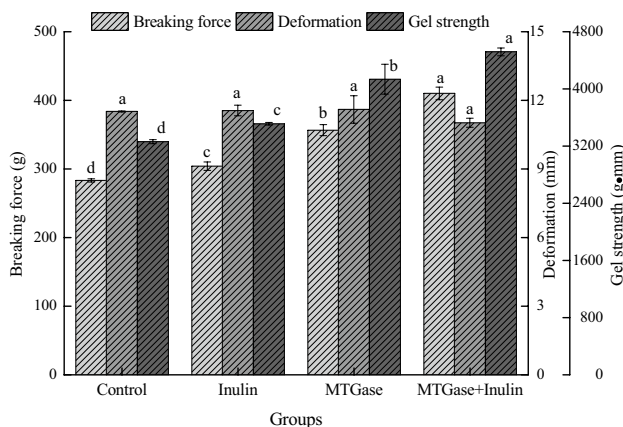


**Fig. 1** Effects of inulin on the breaking force, deformation and gel strength of MTGase-induced silver carp surimi. breaking force, deformation, gel strength. *Control* without inulin and MTGase, *Inulin* inulin with 2.5 g/kg, *MTGase* MTGase with 10 g/kg, *MTGase + inulin* inulin with 2.5 g/kg and MTGase with 10 g/kg. Different lower-case letters (a–d) indicate significant differences ( $P < 0.05$ ) between treatments with breaking force, deformation and gel strength

force and gel strength of the experimental group with 0.25% MTGase, 1% inulin and 0.25% MTGase + 1% inulin were significantly higher than those of the control group ( $P < 0.05$ ), but there were no significant differences in deformation distance ( $P > 0.05$ ). The addition of inulin increased the breaking force and gel strength of silver carp surimi by 7.3% and 7.7%, respectively, when compared with the control group. This variation could be attributed to the chemical composition that inulin possesses abundant hydroxyl groups which significantly affect hydrogen bond [31]. As explored by Sun and Holley [43], this bond is conducive to the formation of three-dimensional network structures. In addition, inulin also likely filled the network gaps in the surimi gel, making the protein structure denser. These results were similar to those observed when 1% konjac glucomannan was added into grass carp fish paste to enhance gel strength [47]. The breaking force and gel strength of the MTGase group were 356.54 and 4135.74 g mm, which increased by 25.9% and 26.8% compared with the control group. The observed increase could be explained by the formation of more  $\epsilon$ -( $\gamma$ -glutamyl) lysine bonds induced by MTGase [8]. The breaking force and gel strength of the 0.25% MTGase + 1% inulin group reached 410.10 and 4518.42 g mm (increased by 44.8% and 38.56% compared with control group), which were higher than those of other groups, indicating that inulin enhanced the ability of MTGase to induce the formation of network structure from myofibrillar proteins. Thus, the utilization of inulin as gel improver may promote the development of surimi products with prebiotic effect in the future [1, 18].

### Textural properties of silver carp surimi gels

The gel texture was mainly compressed twice by simulating the chewing action of the human mouth to obtain parameters corresponding to human sensory evaluation. As shown in Table 2, the hardness, gumminess, chewiness and resilience of the surimi gel of the experimental group were significantly higher than those of the groups without added MTGase and inulin ( $P < 0.05$ ). The results showed

**Table 2** Effects of inulin on the textural properties and WHC of MTGase-induced silver carp surimi

Groups	Hardness (g)	Gumminess	Chewiness (g mm)	Resilience (mm)	Water-holding capacity (%)
Control	3528.17 $\pm$ 41.05 <sup>d</sup>	2614.89 $\pm$ 18.56 <sup>d</sup>	2436.33 $\pm$ 40.61 <sup>d</sup>	0.38 $\pm$ 0.00 <sup>d</sup>	69.48 $\pm$ 1.53 <sup>b</sup>
Inulin	3680.27 $\pm$ 24.46 <sup>c</sup>	2784.91 $\pm$ 7.78 <sup>c</sup>	2597.74 $\pm$ 27.57 <sup>c</sup>	0.41 $\pm$ 0.00 <sup>c</sup>	69.71 $\pm$ 3.49 <sup>b</sup>
TGase	4310.16 $\pm$ 30.60 <sup>b</sup>	3557.70 $\pm$ 30.48 <sup>b</sup>	3414.85 $\pm$ 51.37 <sup>b</sup>	0.49 $\pm$ 0.01 <sup>b</sup>	75.60 $\pm$ 1.80 <sup>a</sup>
TGase + inulin	5155.44 $\pm$ 78.58 <sup>a</sup>	4365.32 $\pm$ 87.83 <sup>a</sup>	4048.63 $\pm$ 64.73 <sup>a</sup>	0.54 $\pm$ 0.07 <sup>a</sup>	76.31 $\pm$ 2.47 <sup>a</sup>

Values are given as mean  $\pm$  SD (standard deviation) from three replications. Different lower case letters indicate the significance of difference amongst mean values in the same column at  $P < 0.05$

Control: without inulin and MTGase; Inulin: inulin with 2.5 g/kg; MTGase: TGase with 10 g/kg; MTGase + Inulin: inulin with 2.5 g/kg and MTGase with 10 g/kg

that inulin could improve the texture characteristics of silver carp surimi gel, probably because soluble dietary fiber could produce the cross-linking with protein after being dissolved in water. This result was consistent with gel strength. In addition, previous study showed that addition of inulin could cause obvious increase in gumminess for oat protein isolate gels prepared at pH 7 [33]. The highest values of textural results appeared in the 0.25% MTGase + 1% inulin group, which suggested that inulin enhanced the MTGase-catalyzed myofibrillar protein gel formation. However, these results were inconsistent with those of a study conducted by Cardoso et al. [7]. This difference may be related to the degree of polymerization, the amount of inulin and the gel properties of different species of fish.

### WHC of silver carp surimi gels

Water holding capacity refers to the ability of proteins to bind water, and changes in WHC influence the color, flavor, tenderness and taste of heat-induced gel [20]. As shown in Table 2, there were no significant ( $P > 0.05$ ) differences in WHC between the 1% inulin group and the control group. This could ascribe to the water-soluble polysaccharide inulin filling in the pores between proteins, which hindered the complete combination of water molecules and proteins and decreased the proportion of free water flowing inside the surimi gel. As a result, water loss and WHC are relatively low during the centrifugal process.

There were significant differences ( $P < 0.05$ ) in WHC between the control group and MTGase or MTGase + inulin group, and the WHC of latter groups were higher than that of the control group and the inulin group. The reason behind this difference was that water could be better trapped into the dense, uniform gel network of MTGase and MTGase + inulin group, resulting in higher WHC [11]. The gel strength and textural properties provided clear evidence (Fig. 1; Table 2).

To further analyze the relationships among gel strength, texture properties, and WHC, we performed the Pearson correlation and the corresponding results are presented in Table 3. Apart from deformation, the breaking force was correlated significantly with gel strength, hardness, gumminess, chewiness, resilience and WHC, indicating the gel strength, texture and WHC are interrelated. In this paper, however, there existed no correlation between deformation and other properties, which further proven the deformation could not be the critical factor affecting the gel properties of gel from MTGase, inulin or MTGase + inulin groups.

### Dynamic rheology of silver carp surimi gels

Changes in the rheological behavior of silver carp surimi gel formed by heating were identified by dynamic rheology, the change curve is shown in Fig. 2. In this study, we measured the storage modulus ( $G'$ ), the loss modulus ( $G''$ ) and the damping factor ( $\tan \delta$ ), which stand for the elastic properties of the surimi gel, the viscous properties of the surimi gel and the ratio of  $G''/G'$ , respectively [15]. The dynamic rheology reflects the rheological properties and gel properties of surimi gel [46].

The rheological changes in surimi gel can be explained by the structural changes and interactions of myosin.  $G'$  became larger as temperature increased from 20 to 30 °C. This was likely because the interaction between protein molecules at low temperatures increases the viscoelasticity of the sample [25, 46]. The decrease in  $G'$  with temperature increased from 30 to 52 °C may occurred for the following reasons: (i) myosin was degraded by the endogenous proteolytic enzymes of the fish, (ii) myosin tail expansion led to destruction of the protein network, and (iii) hydrogen bonding decreased during heating [30]. At temperatures above 52 °C, the protein re-aggregated and formed cross-links, resulting in a flexible three-dimensional network structure [44]. The changes in  $G''$  were similar to those in  $G'$ , but the  $G''$

**Table 3** Correlation analysis of various gel indexes among different groups

Indexes	Breaking force	Deformation	Gel strength	Hardness	Gumminess	Chewiness	Resilience	Water-holding capacity
Breaking force	1.000	-0.529	0.975**	0.986**	0.988**	0.978**	0.991**	0.746**
Deformation		1.000	-0.329	-0.486	-0.469	-0.386	-0.454	-0.249
Gel strength			1.000	0.971**	0.978**	0.989**	0.986**	0.767**
Hardness				1.000	0.998**	0.987**	0.984**	0.781**
Gumminess					1.000	0.993**	0.992**	0.799**
Chewiness						1.000	0.992**	0.818**
Resilience							1.000	0.805**
Water-holding capacity								1.000

\*\*Significance of difference amongst various gel indexes at  $P < 0.01$

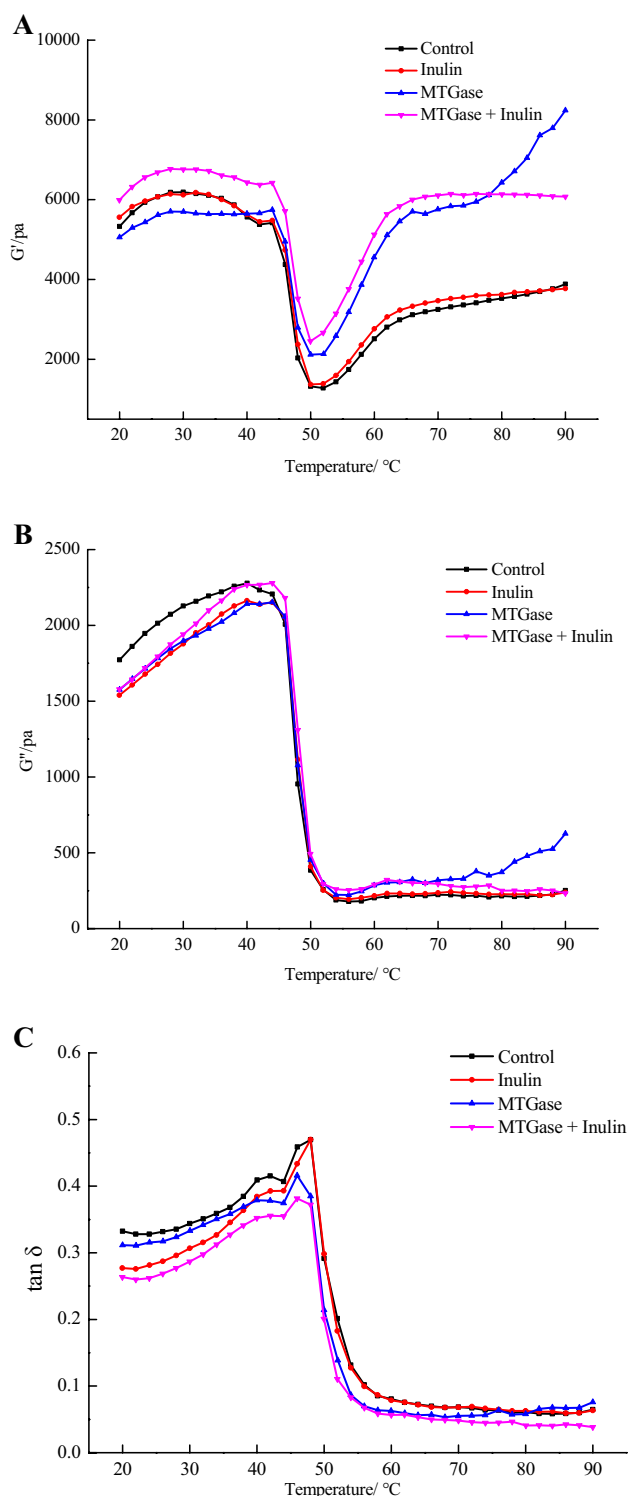


**Fig. 2** Effects of inulin on dynamic rheology of MTGase-induced silver carp surimi. **a–c** Storage modulus ( $G'$ ), loss modulus ( $G''$ ), damping factor ( $\tan \delta$ ), respectively. *Control* without inulin and MTGase, *Inulin* inulin with 2.5 g/kg, *MTGase* MTGase with 10 g/kg, *MTGase + inulin* inulin with 2.5 g/kg and TGase with 10 g/kg

value was much lower than that of  $G'$ , indicating that the elastic composition played a dominant role in the formation of surimi gel.

The trends in dynamic rheological curves of the four groups were similar, but the final  $G'$ ,  $G''$  and  $\tan \delta$  values were different. In general, the values of  $G'$  and  $G''$  of the experimental groups, including inulin, MTGase and MTGase + inulin groups, were significantly greater than that of the control group, and the experimental group with MTGase + inulin had the greatest values. The  $\tan \delta$  values of MTGase + inulin group is lowest, indicating elastic properties of MTGase + inulin group is most significant compared with other groups. This might because of the interaction of inulin with proteins, forming disulfide bonds and inducing MTGase to form more  $\epsilon$ -( $\gamma$ -glutamyl) lysine bonds. The high  $G'$  values indicated the enhancement of the surimi gel properties and the low  $\tan \delta$  values referred to a highly elastic network structure, which is coincided with the gel strength shown in Fig. 1.

### Protein secondary structure of silver carp surimi gels

Raman spectroscopy is a useful and reliable approach to investigate protein conformation and the molecular interactions between additives and proteins in a wide range of food domains. This technique can reflect changes in the molecular structure of substances according to the relative strength and frequency of amino acid side chains, polypeptides and polysaccharide skeleton vibrations [39]. The Raman spectra of protein is depicted in Fig. 3a, Amides I and III are the main characteristics of the protein conformation peaks, where phenylalanine is used as a standard peak of protein conformation. Figure 3b shows the changes in protein secondary structure, in which, the number of emergent  $\alpha$ -helix gradually decreased, the content of  $\beta$ -sheet and  $\beta$ -turn gradually increased, and there were no significant differences in the content of random coil. These changes may have occurred because the structure of  $\alpha$ -helix unfolded and  $\beta$ -sheet and  $\beta$ -turn formed through the interaction of hydrophobic residues exposed between molecules [27, 29]. Zhuang et al. [56] once showed that the texture of the sample was negatively correlated with the  $\alpha$ -helix content and positively correlated with the  $\beta$ -sheet,  $\beta$ -turn and random coil content. The gel properties of the experimental groups treated with inulin, MTGase and MTGase + inulin were better than that of the control group. The main reason of this was the existence of MTGase and inulin affected protein conformation. MTGase changes the structure of myosin heavy chain by cross-linking and reduces the  $\alpha$ -helix content, thereby increasing the percentage of  $\beta$ -sheet and forming a high molecular weight polymer and therefore a better gel [26]. The experimental group with MTGase + inulin showed the best results, indicating

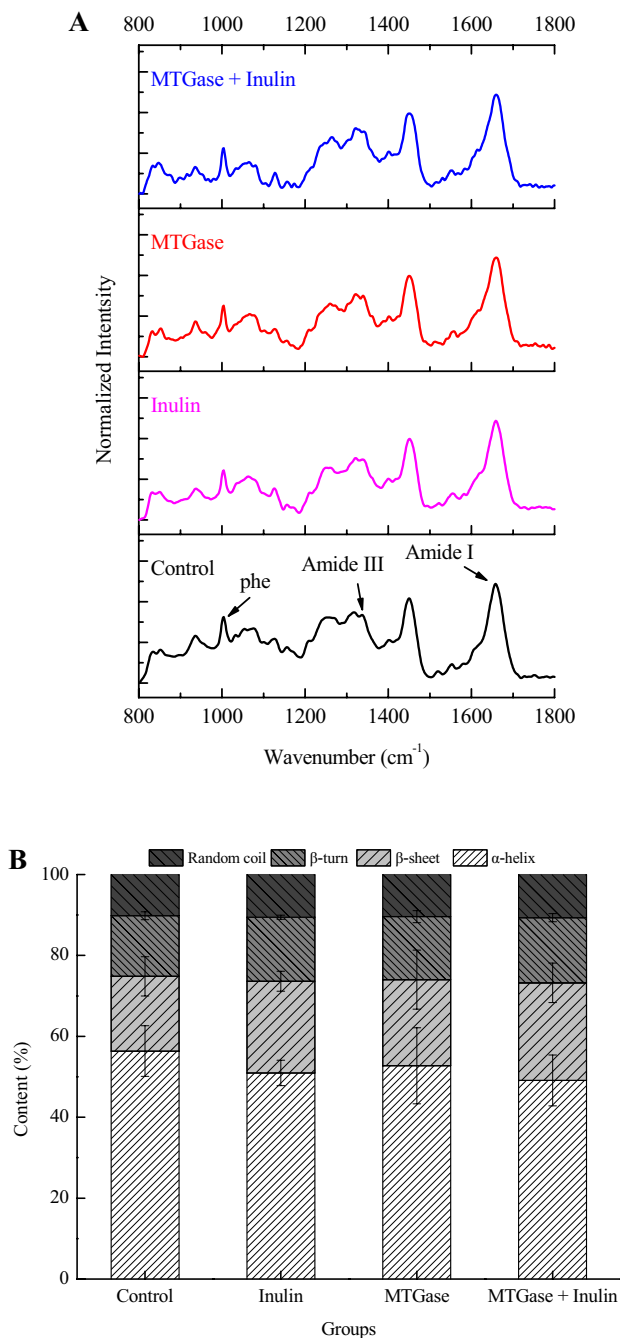


**Fig. 3** Effects of inulin on the protein secondary structure of MTGase-induced silver carp surimi. **a** Raman spectra ( $800\text{--}1800\text{ cm}^{-1}$ ) and **b** protein secondary structure of different treatments,  $\alpha$ -helix contents,  $\beta$ -sheet contents,  $\beta$ -turn contents, Random coil contents. *Control* without inulin and MTGase, *Inulin* inulin with 2.5 g/kg, *MTGase* MTGase with 10 g/kg, *MTGase + inulin* inulin with 2.5 g/kg and MTGase with 10 g/kg

that the inulin and MTGase synergistically promoted the formation of a uniform three-dimensional network structure of the surimi gel.

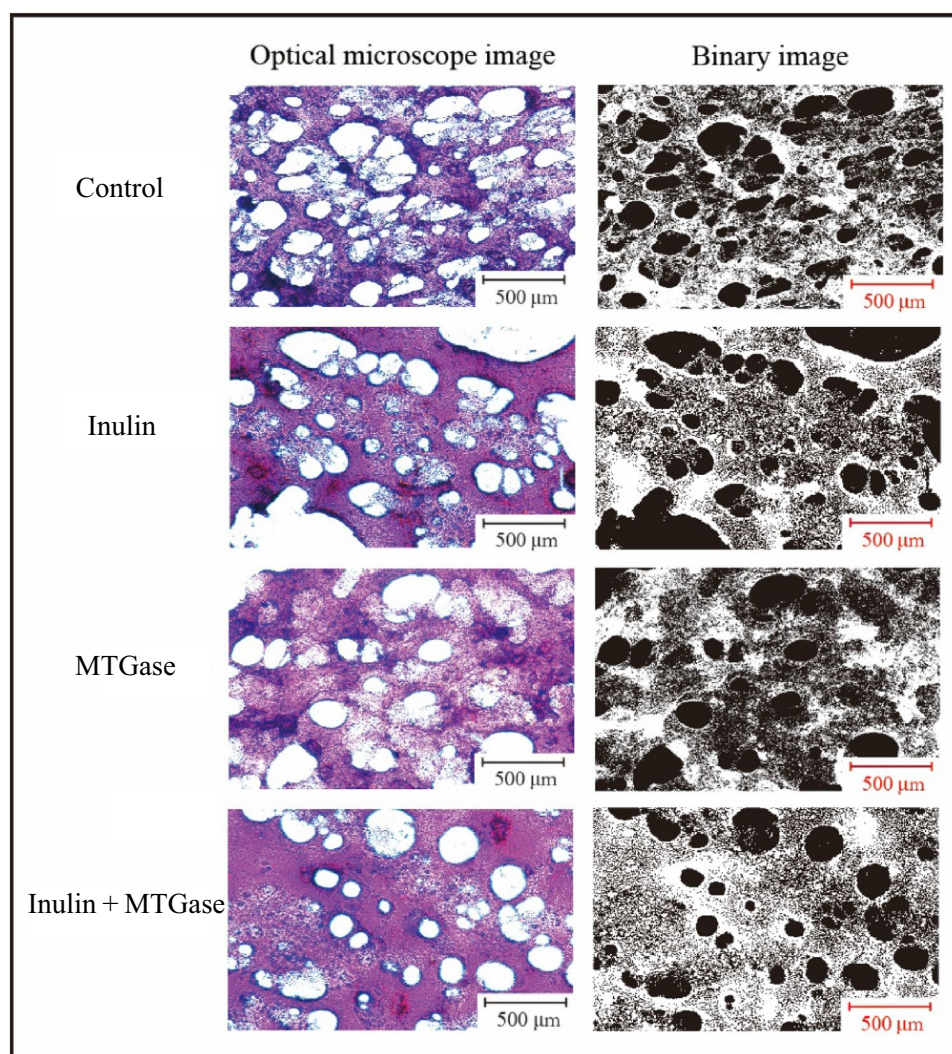
## Microstructure of silver carp surimi gels

Light microscopy combined with staining is a visual mean of obtaining information about gel microstructure, which has been widely applied in surimi gelation chemistry. As shown in Fig. 4, cavities with different sizes and numbers in the blended gels can be observed through the optical microscope image, and the binary image obtained by Image J software can clearly reveal the change of the pores in each experimental group. The microstructure of the surimi gels in the control was relatively loose and non-heterogeneous, with many large pores. This could be attributed to damage to the protein network caused by free water migration, illustrating the poor ability of the gel structure to bind water in this group (Fig. 4). Meanwhile, this spongy structure demonstrated the heating-induced gel forming ability of silver carp surimi was poor, in accordance with rheological and textural results (Fig. 2; Table 2). However, the network of gels containing inulin was comparable, consisting of compact and homogeneous microstructures accompanied by small pore dimensions, compared with the control. Gravelle et al. [17] showed that hydrophilic fillers could improve the surimi gel and reduce the formation of water channels in the gel network. Above all, the most continuous and closed network was exhibited by MTGase groups containing hydrocolloid inulin. The results might be because of cross-linking of proteins induced by MTGase and localized interactions involving hydrogen and hydrophobic bonding from good filler inulin and proteins during the processing of surimi gels [16, 55]. Moreover, binding more water would decrease the protein/water ratio after dissolution of inulin, which was necessary for the formation of a stronger gel during thermal treatment. Alternatively, under MTGase + inulin conditions, the gels had a completer and more continuous microstructure than in the other three groups, which supported the idea that inulin had a synergistic effect on MTGase-induced cross-linking of protein and further enhanced the gel properties of silver carp surimi.

## Protein pattern of silver carp surimi gels

SDS-PAGE can directly analyze the cross-linking, aggregation and degradation of proteins at the molecular level [49]. It is well known that myosin heavy chain (MHC) plays a pivotal role in shaping the gel microstructure. Additionally, as reported by Samejima et al. [37], although actin (AC) cannot form gel, it is able to react with MHC to enhance gel elasticity. Thus, it makes sense to analyze changes in MHC and AC bands of all groups. As can be seen from Fig. 5a, c, the MHC bands of the MTGase, inulin and MTGase + inulin groups were shallower than those of the control group. Among these, the MHC bands of the MTGase + inulin experimental group had the smallest integrated density. Concomitantly,

**Fig. 4** Effects of inulin on the microstructure of MTGase-induced silver carp surimi. *Control* without inulin and MTGase (400 ×), *Inulin* inulin with 2.5 g/kg (400 ×), *MTGase* MTGase with 10 g/kg (400 ×), *MTGase + inulin* inulin with 2.5 g/kg and MTGase with 10 g/kg (400 ×)



MHC formed polymers (top of the gel) through cross linking. It indicated that inulin could enhance the cross-linking effects of MTGase on myosin heavy chains. An investigation had shown that polysaccharides may promote the formation of more  $\epsilon$ -( $\gamma$ -glutamyl) lysine bonds by MTGase [20]. Benjakul et al. [5] also confirmed that chitosan and MTGase can enhance the gel strength of surimi by protein–protein and protein–chitosan conjugates. Based on the results shown in Fig. 5b, c, plenty of aggregates on the top of the concentrated gum were reduced and integrated MHC density were intensified after adding  $\beta$ -mercaptoethanol. This disclosed that disulfide bonds were primarily responsible for the crosslinking of surimi gels containing inulin. However, the lower MHC density of MTGase and MTGase + inulin groups indicated that the  $\epsilon$ -( $\gamma$ -glutamyl) lysine bond played a major role in the formation of surimi gel. Apart from MHC bands, we found that the AC bands of inulin group undergone large changes from Fig. 5, implying which might participate in the formation of gel in this study. In short, there

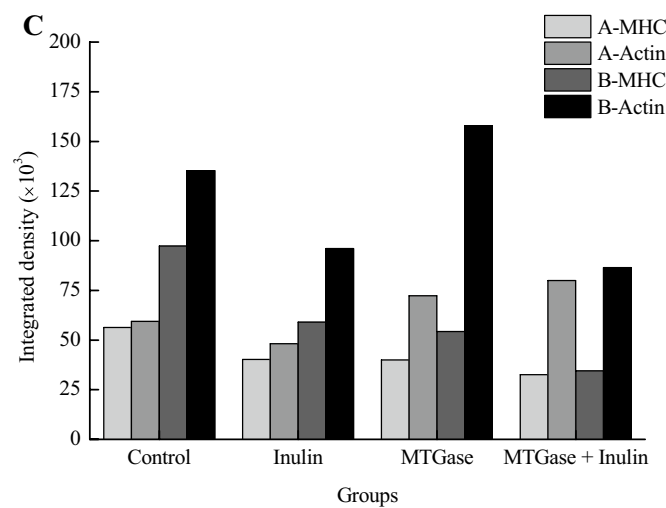
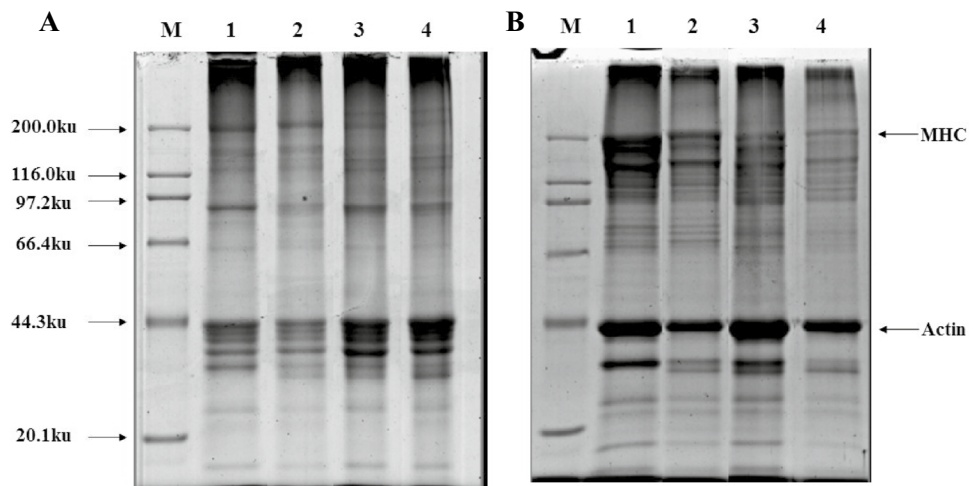
existed consistency among changes in MHC, AC bands and gel properties.

### Proposed mechanisms

From all results of this study, we found that inulin, MTGase and incorporation of inulin and MTGase had the ability to ameliorate the gel properties of sliver surimi during heating process. However, only inulin was added into sliver surimi, the gel strength was lower than that of MTGase and MTGase/inulin group (Fig. 1). This difference proven the action of inulin was not consistent with MTGase, it might be distributed in gel network structure acting as filler. In addition, Kim et al. [21] also reported that when the concentration of inulin decreased to 5% (w/v), inulin could not form gel network in the water system due to lacking particle and molecular effect. However, of note is that MTGase can induce the  $\epsilon$ -amino group located in the lysine residue and the  $\gamma$ -amide group situated in glutamine residue to generate



**Fig. 5** Effects of inulin on SDS-PAGE of MTGase-induced silver carp surimi. **a** Without  $\beta$ -mercaptoethanol, **b** with  $\beta$ -mercaptoethanol; *M* maker, *MHC* heavy chain of myosin, and **c** integrated density, A-MHC, A-Actin, B-MHC, B-Actin. Bands 1–4 means Control, Inulin, MTGase and MTGase + Inulin. Control without inulin and MTGase, *Inulin* inulin with 2.5 g/kg, *MTGase* MTGase with 10 g/kg, *MTGase + inulin* inulin with 2.5 g/kg and MTGase with 10 g/kg



an  $\epsilon$ -( $\gamma$ -glutamyl) lysine bond, further leading to cross-linking between proteins. As shown in Fig. 2,  $G'$ ,  $G''$  and  $\tan \delta$  curve are basically conformal in control and inulin group, indicating also inulin barely changes the protein molecular orientation and protein-protein interactions during this process. According to Fig. 3 and Table 2, it was clear that the gel of inulin treatment had better water holding capability than that of control group, which could be explained by the stronger water-binding ability of inulin [11]. Besides, the three-dimension network of MTGase and MTGase/inulin groups was well-linked and connected and free water could be trapped in gel structure. Likewise, we reached the same conclusions from SDS-PAGE patterns and the secondary structure of MP. Therefore, proposed mechanisms of effects of inulin or the synergistic combination of inulin and MTGase on the gel properties were disclosed in Fig. 6. In this model system, the present of inulin was beneficial to gel network due to moisture absorption property and filling effect. MTGase played a critical role in promoting gel formation, rather than the action of inulin. However, it was worth

noting that the filling effect of inulin facilitated cross-linking formation induced by MTGase of silver carp surimi gel via affecting protein aggregation and conformation.

## Conclusions

The results of this study indicated that the incorporation of MTGase and inulin into silver carp surimi gels significantly increased water retention and improved textural characteristics such as hardness, resilience, cohesiveness, and springiness. Meanwhile, MTGase and inulin both produced gel matrices with homogeneous and continuous networks, especially when MTGase and inulin existed together. Dynamic rheology diagrams showed that the experimental group with inulin + MTGase had the highest  $G'$ , indicating that inulin could cooperate with MTGase to promote better formation of the surimi gel network structure. The two additives significantly influenced the secondary structural arrangement of the protein, resulting in the conversion of

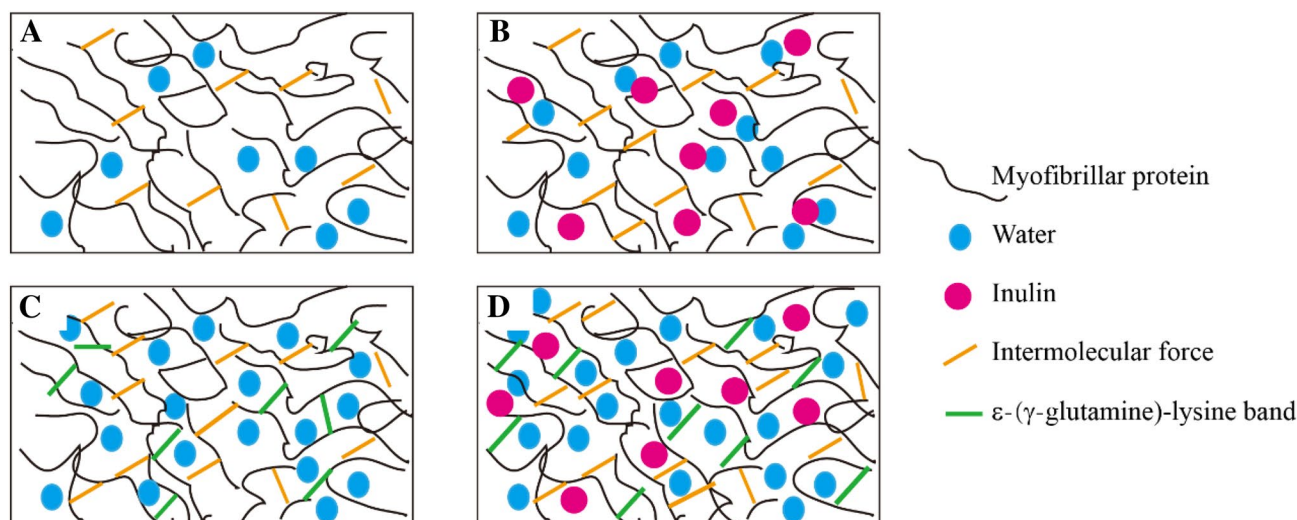


**Fig. 6** Proposed mechanisms for the formation of gel network induced by inulin and MTGase. **a** Control group without inulin and MTGase, **b** inulin group, **c** MTGase group and **d** MTGase + Inulin

group. *Control* without inulin and MTGase, *Inulin* inulin with 2.5 g/kg, *MTGase* TGase with 10 g/kg, *MTGase + inulin* inulin with 2.5 g/kg and MTGase with 10 g/kg

$\alpha$ -helices to  $\beta$ -sheets and  $\beta$ -turns, benefiting the formation of gels. The acceleration was further supported by SDS-PAGE analysis, which demonstrated the presence of MTGase and inulin increased the cross-linking of MHC bands during the process of gelation. Thus, the results lend credence to the modifications of gel properties research in freshwater fish and simultaneously suggest that the application of nutritional, soluble dietary fibers may be a useful way to improve the textural properties of surimi gels.

**Acknowledgements** This study was supported by the Key Laboratory of Refrigeration and Conditioning Aquatic Products Processing, Ministry of Agriculture (KLRCAPP2018-12), the Natural Science Foundation of Liaoning Province (20180550889), Liaoning Revitalization Talents Program (XLYC1907040, 1807133), and National Natural Science Foundation of China (31972107, 31701631, 31771999).

### Compliance with ethical standards

**Conflict of interest** No potential conflict of interest was reported by the authors.

### References

- M.B. Akin, M.S. Akin, Z. Kirmaci, *Food Chem.* **104**(1), 93–99 (2007)
- F. Alakhrash, U. Anyanwu, R. Tahergorabi, *LWT Food Sci. Technol.* **66**, 41–47 (2016)
- Y. An, J. You, S. Xiong, T. Yin, *Food Chem.* **257**, 216–222 (2018)
- B. Bchir, N. Sadin, S.N. Ronkart, C. Blecker, *Colloid Polym. Sci.* **297**(6), 849–860 (2019)
- S. Benjakul, W. Visessanguan, S. Phatchrat, M. Tanaka, *J. Food Biochem.* **27**(1), 53–66 (2003)
- M.B. Canalis, A.E. León, P.D. Ribotta, *Food Chem.* **271**, 309–317 (2019)
- C. Cardoso, R. Mendes, P. Vaz-Pires, M.L. Nunes, *J. Sci. Food Agric.* **89**(10), 1648–1658 (2009)
- C. Cardoso, R. Mendes, P. Vaz-Pires, M.L. Nunes, *LWT Food Sci. Technol.* **44**(5), 1282–1290 (2011)
- C. Cardoso, B. Ribeiro, R. Mendes, *J. Food Eng.* **113**(4), 520–526 (2012)
- D.V. Carvalho, L.M.A. Silva, E.G. Alves Filho, F.A. Santos, R.P. de Lima, A.F.S.C. Viana et al., *Food Funct.* **10**(3), 1671–1683 (2019)
- S. Chanarat, S. Benjakul, *Food Chem.* **136**(2), 929–937 (2013)
- J. Chen, T. Deng, C. Wang, H. Mi, S. Yi, X. Li, J. Li, *J. Sci. Food Agric.* **100**(5), 2252–2260 (2020)
- A. Debusca, R. Tahergorabi, S.K. Beamer, S. Partington, J. Jaczynski, *Food Chem.* **141**(1), 201–208 (2013)
- A. Debusca, R. Tahergorabi, S.K. Beamer, K.E. Matak, J. Jaczynski, *Food Chem.* **148**, 70–76 (2014)
- B. Egelandsdal, B. Martinsen, K. Autio, *Meat Sci.* **39**(1), 97–111 (1995)
- A.L.C. Gaspar, S.P. de Góes-Favoni, *Food Chem.* **171**, 315–322 (2015)
- A.J. Gravelle, S. Barbut, A.G. Marangoni, *Sci. Rep.* **7**(1), 1–16 (2017)
- J.T. Guimarães, C.F. Balthazar, R. Silva, R.S. Rocha, J.S. Graça, E.A. Esmerino et al., *Curr. Opin. Food Sci.* **33**, 38–44 (2020)
- X. Guo, L. Shi, S. Xiong, Y. Hu, J. You, Q. Huang, T. Yin, *LWT* **99**, 105–111 (2019)
- Y. Hu, W. Liu, C. Yuan, K. Morioka, S. Chen, D. Liu, X. Ye, *Food Chem.* **176**, 115–122 (2015)
- Y. Kim, M.N. Faqih, S.S. Wang, *Carbohydr. Polym.* **46**(2), 135–145 (2001)
- M. Kiumarsi, M. Shahbazi, S. Yeganehzad, D. Majchrzak, O. Lieleg, B. Winkeljann, *Food Chem.* **277**, 664–673 (2019)
- Y. Kumazawa, T. Numazawa, K. Seguro, M. Motoki, *J. Food Sci.* **60**(4), 715–717 (1995)
- M.G. Kuntz, G.M. Fiates, E. Teixeira, *Br. Food J.* **115**(2), 235–251 (2013)

25. F. Lefevre, B. Fauconneau, A. Ouali, J. Culioli, *J. Food Sci.* **63**(2), 299–304 (1998)
26. T. Lesiow, G.K. Rentfrow, Y.L. Xiong, *Meat Sci.* **128**, 40–46 (2017)
27. C.E. Li, S. Nakai, M. Hirotsuka, *Raman Spectroscopy as a Probe of Protein Structure in Food Systems* (Blackie Academic and Professional, London, 1994), pp. 163–184
28. W. Li, J. Zhang, C. Yu, Q. Li, F. Dong, G. Wang, G. Gu, Z. Guo, *Carbohydr. Polym.* **121**, 315–319 (2015)
29. E. Li-Chan, S. Nakai, *J. Agric. Food Chem.* **39**(7), 1238–1245 (1991)
30. R. Liu, S.M. Zhao, S.B. Xiong, B.J. Xie, H.M. Liu, *J. Food Sci.* **72**(7), E399–E403 (2007)
31. J. Liu, D. Luo, X. Li, B. Xu, X. Zhang, J. Liu, *Food Chem.* **210**, 235–241 (2016)
32. Ministry of Agriculture, *China Fishery Statistical Yearbook* (China Agricultural Press, Beijing, 2019)
33. T.V. Nieto-Nieto, Y.X. Wang, L. Ozimek, L. Chen, *Food Hydrocoll.* **50**, 116–127 (2015)
34. C. Qiu, W. Xia, Q. Jiang, *Food Res. Int.* **52**(1), 199e205 (2013)
35. M.B. Roberfroid, *J. Nutr.* **129**(7), 398–401 (1999)
36. J. Rodríguez-García, A. Salvador, I. Hernando, *Food Bioprocess Technol.* **7**(4), 964–974 (2014)
37. K. Samejima, Y. Hashimoto, T. Yasui, T.T. Fukazawa, *J. Food Sci.* **34**(3), 242–245 (1969)
38. I. Sánchez-González, P. Carmona, P. Moreno, J. Borderías, I. Sanchez-Alonso, A. Rodríguez-Casado, M. Careche, *Food Chem.* **106**(1), 56–64 (2008)
39. I. Sánchez-González, A. Rodríguez-Casado, M. Careche, P. Carmona, *Food Chem.* **112**(1), 162–168 (2009)
40. M.G. Saraç, M. Dogan, *Eur. Food Res. Technol.* **242**(8), 1331–1342 (2016)
41. N. Seki, H. Uno, N.H. Lee, I. Kimura, K. Toyoda, *Nippon Suisan Gakk* **56**(1), 125–132 (1990)
42. M. Shoaib, A. Shehzad, M. Omar, A. Rakha, H. Raza, H.R. Sharif, A. Shakeel, A. Ansari, S. Niazi, *Carbohydr. Polym.* **147**, 444–454 (2016)
43. X.D. Sun, R.A. Holley, *Compr. Rev. Food Sci. F* **10**(1), 33–51 (2011)
44. H. Wang, M. Pato, Z. Pietrasik, P. Shand, *Food Chem.* **113**(1), 21–27 (2009)
45. M. Wu, Y.L. Xiong, J. Chen, X. Tang, G. Zhou, *J. Food Sci.* **74**(4), E207–E217 (2009)
46. Y.L. Xiong, S.P. Blanchard, *J. Food Sci.* **59**(4), 734–738 (1994)
47. G. Xiong, W. Cheng, L. Ye, X. Du, M. Zhou, R. Lin, S. Geng, M. Chen, H. Corke, Y.Z. Cai, *Food Chem.* **116**(2), 413–418 (2009)
48. W. Xu, Y. Xiong, Z. Li, D. Luo, Z. Wang, Y. Sun, B.R. Shah, *Food Hydrocoll.* **105**, 105772 (2020)
49. J. Yang, Y.L. Xiong, *Food Chem.* **243**, 231–238 (2018)
50. S. Yi, Y. Huo, C. Qiao, W. Wang, X. Li, *J. Food Sci.* **84**(12), 3634–3641 (2019)
51. T. Yin, R. Yao, I. Ullah, S. Xiong, Q. Huang, J. You, Y. Hu, L. Shi, *LWT* **111**, 111–116 (2019)
52. H. Zhang, Y. Xiong, A.M. Bakry, S. Xiong, T. Yin, B. Zhang, J. Huang, Z. Liu, Q. Huang, *Food Hydrocoll.* **88**, 256–264 (2019)
53. Z. Zhu, O. Bals, N. Grimi, E. Vorobiev, *Int. J. Food Sci. Technol.* **47**(7), 1361–1368 (2012)
54. Z. Zhu, T.C. Lanier, B.E. Farkas, B.S. Li, *J. Food Eng.* **131**, 154–160 (2014)
55. X. Zhuang, W. Zhang, R. Liu, Y. Liu, L. Xing, M. Han, Z. Kang, X.L. Xu, G.H. Zhou, *Food Res. Int.* **100**, 586–594 (2017)
56. X. Zhuang, M. Han, Y. Bai, Y. Liu, L. Xing, X.L. Xu, G.H. Zhou, *Food Hydrocoll.* **74**, 219–226 (2018)
57. X. Zhuang, X. Jiang, H. Zhou, Y. Chen, Y. Zhao, H. Yang, G. Zhou, *Carbohydr. Polym.* **229**, 115449 (2020)

**Publisher's Note** Springer Nature remains neutral with regard to jurisdictional claims in published maps and institutional affiliations.